京都大学大学院理学研究科附属天文台技報
Technical Reports from Astronomical Observatory
Graduate School of Science, Kyoto University

Vol. 6-3

Update of the Spectro-polarimeter on the Domeless Solar Telescope at Hida Observatory

Kiyoshi Ichimoto[1], Yuwei Huang[1], Daiki Yamasaki[1], Goichi Kimura[1], Denis Cabezas[1], Tomoko Kawate[2], and Satoru Ueno[1]

2022年 12月23日 submitted

1. Astronomical Observatory, Kyoto University, Kitashirakawa-oiwake-cho, Kyoto 606-8502, Japan
2. National Institute for Fusion Science, 322-6 Oroshi-cho, Toki, Gifu 509-5292 Japan

Abstract:

A new spectro-polarimeter was installed on the Domeless Solar Telescope at Hida Observatory. Major updates from the previous system are as follows; a super achromatic dual beam polarimeter, communication interface between telescope and data acquisition PC for image scanning, flexible setup for observing a wavelength range of 500-1100 nm, and a high sensitivity infrared camera. The field of view of the system is 120arcsec along the slit of spectrograph, and with a slit width of 0.64 arcsec, the system can achieve a sensitivity of $3x10^{-4}$ in a few second in on-disk observation. Details of the instruments, the data reduction flow and initial results obtained by the new system are presented. At the end, future prospect is also discussed.

1. Introduction

The spectro-polarimeter is a key equipment for modern solar observatories for the research of the solar magnetism and advanced physical diagnosis by sensing polarization signals in solar spectrum. In this paper, we report the recent development of the spectro-polarimeter on the Domaless Solar Telescope (DST, Nakai and Hattori 1985) at Hida Observatory of Kyoto University.

The DST is a 60cm aperture vacuum solar telescope mounted on a tower of 22m high. It is equipped with two spectrographs; One is the vertical spectrograph, which is installed in a 15m long vacuum tank and used for high dispersion (up to $\lambda/\Delta\lambda \sim 10^6$) spectroscopic observations in a single wavelength window. The other is the horizontal spectrograph, which allows us to perform multi-wavelength observations with highly flexible combinations of spectral windows.

So far, we have constructed a series of spectro-polarimeters on the DST. The first generation installed on the vertical spectrograph was dedicated for observations in FeI630.2 nm line with a step-wise rotating quarter-

waveplate (Kiyohara etal. 2004). The second generation was also installed on the vertical spectrograph, but, with a continuous rotation of an achromatic waveplate and a high frame rate camera, it enabled us to achieve a higher sensitivity in a wavelength window selected from the range of 500 – 1100 nm (Anan etal 2012). The third generation was equipped on the horizontal spectrograph and it allowed us to make multi-wavelength observations (Anan etal 2018). The new spectro-polarimeter presented in this paper is the fourth generation. The major updates from the previous system are as follows; (1) it is usable on both vertical and horizontal spectrographs, (2) the polarimeter is renewed with a 50mm diameter super achromatic waveplate mounted in a new rotating mechanism, (3) communication interfaces between the DST control system and data acquisition PC are established to control the angle of a mirror in DST for image scanning and to record the DST attitude information in the data acquisition PC for the purpose of the later data calibration, (4) installation of a high sensitivity near infrared camera.

In the following sections, we present the details of the new system (Sec.2), data calibration flow (Sec.3), some examples of obtained data (Sec.4), and future prospect (Sec.5).

2. The updated polarimeter system

Figure 1 shows the overall constitution of DST and the spectro-polarimeter.

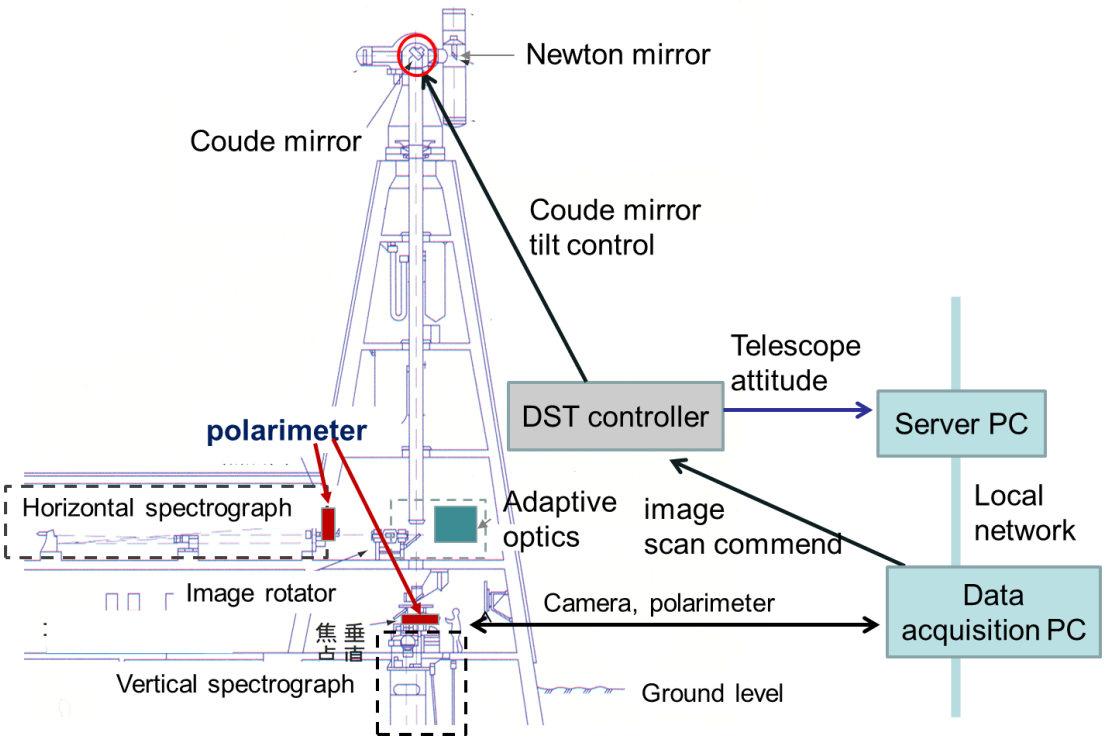

Figure 1. Constitution of DST spectro-polarimeter

2.1 Polarimeter

The polarimeter consists of a rotating waveplate and a polarizing beam splitter assembly. It is mounted just behind the entrance slit of the spectrographs, i.e., in a beam of DST secondary focus with F/53. The waveplate for modulating the polarization is Panchanratnan type with a 5-layer stack of polymer retarder (Hi-Retax 310nm, LUCEO). The diameter is 50mm and it has nearly constant retardation of about 127° over the wavelength range of 500 – 1100 nm (Figure 2). The rotating stage (HST-120YAW-0B, SIGMAKOKI) accommodating the waveplate is driven by a stepping motor with the highest speed of 2 revolutions per second. The speed of the rotation can be chosen flexibly depending on the exposure time of the camera. The rotating stage has an origin sensor, that generates a pulse signal when the edge of a plate on the roter passes the sensor.

The polarization analyzer following the rotating waveplate is an assembly of 5 beam splitter cubes, one of which is a wideband polarizing

beam splitter with a multilayer coating in it (SIGMAKOKI) (figure 3). The diattenuation shown in figure 3 demonstrates its superior performance as a polarization analyzer over the wavelength range of 500 – 1100 nm except a partial defect around 750 nm. The diagonal size of the polarizing beam splitter limits the field of view of the polarimeter, i.e., the length of the slit of the spectrograph needs to be 20 mm, which corresponds to 127 arcsec on the sky (figure 3a). The two beams exiting from the polarization analyzer are linearly polarized in the directions of ±45° with respect to the slit. In order to compensate the displacement of the exiting beams in direction perpendicular to the slit, a rhombus prism (Morita optics) is attached at the exit of the beam splitter assembly. On all optical surfaces in the polarimeter, a wideband anti-reflection coating is deposited.

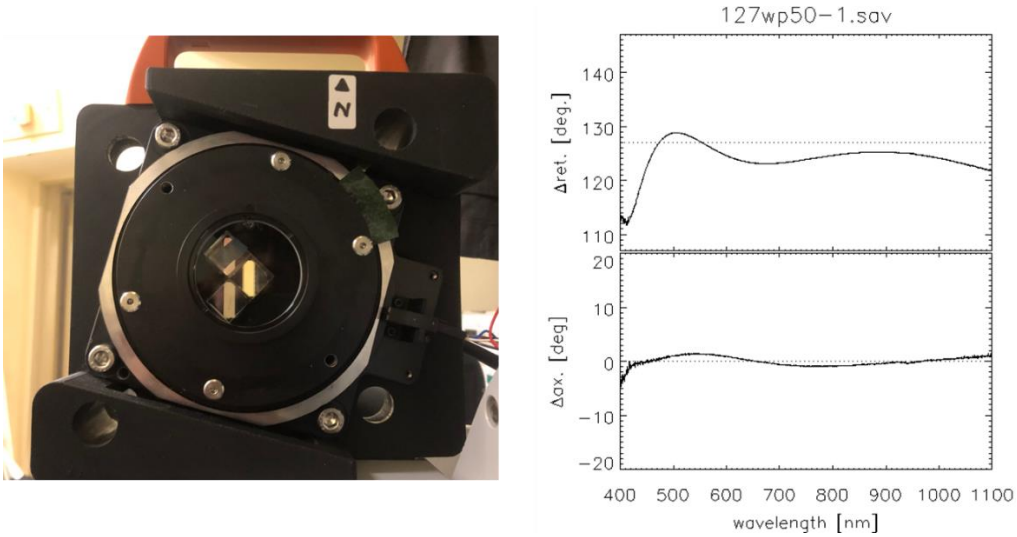

Figure 2. Polarization modulator (left) and characteristics of the waveplate (right). The top of the right panel shows the retardation of the waveplate and bottom shows the orientation of the retardation axis against the wavelength. The data was obtained by the Mueller Matrix Spectro-polarimeter (Ichimoto etal. 2006).

The housing accommodating the rotating waveplate and polarizing beam

splitter assembly was fabricated in house by a 3D printer with plastic material.

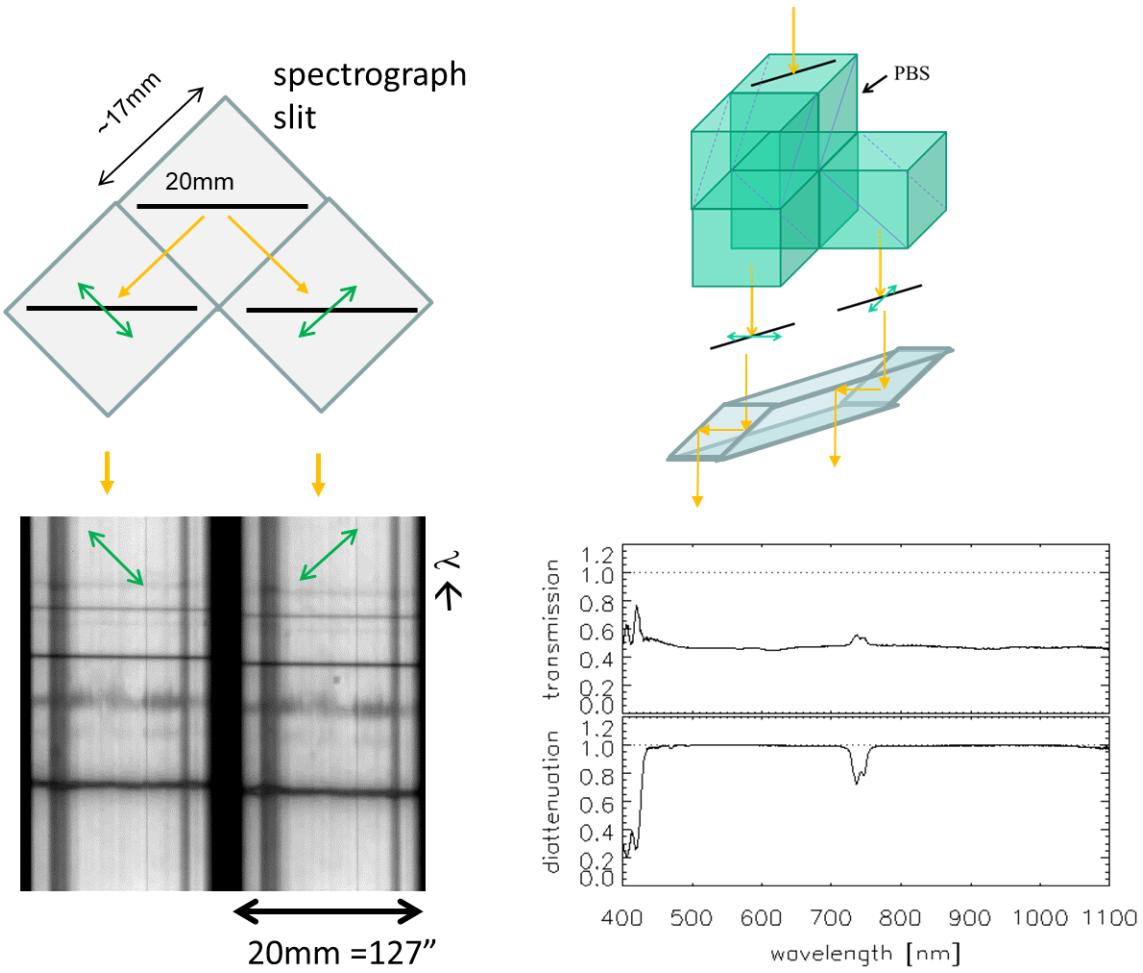

Figure 3. Polarization analyzer consisting of a cube assembly and beam shifting rhombus prism. Bottom left is an example of spectral image with arrows indicating the direction of the linear polarization of the two spectra. Bottom right shows the transmission and diattenuation of the polarizing beam splitter against the wavelength.

2.2 Communication interface between DST and data acquisition PC

DST has a capability for manipulating the tilt angle of the Coude mirror that feeds the light from the secondary mirror of the Gregorian telescope to the focus at the entrance slit of the spectrographs in observing rooms.

Responding to a digital signal from the operation console, the control software of DST tilts the Coude mirror to shift the solar image in direction perpendicular to the slit. We added an electrical harness to connect the DST operation console and a digital IO device (DIO-3232LX-USB, CONTEC) that is connected to the data acquisition PC via USB (see figure 1). Through this line, the data acquisition PC can shift the image on the slit stepwise in synchronous with the data acquisition. Note that, since the driving mechanism of the Coude mirror of DST is an analog system, the repeatability of the slit position on the solar image is not sufficiently good, so it is recommended to reset the Coude mirror to its mechanical origin before the start of each scanning observation. Minimum step size from experiments is approximately 1.38 arcsec on the sky.

The Mueller matrix of DST changes in a day according to the pointing attitude of the telescope on the alto-azimuth mount and the orientation of the slit (i.e. the polarimeter) with respect to the telescope. Therefore information of the telescope attitude and the orientation of the slit at the time of data acquisition is needed for calibrating the instrumental polarization in the data reductions. Such information is acquired from the bus line connecting the control computer and driving electronics of DST to the data acquisition PC through a digital IO device at a rate of 20 Hz, and they are recorded in a fits extension header of each observation data set.

2.3 Imaging sensors

For our spectro-polarimeter, two cameras are available. One is a visible camera (ORCA-4, Hamamatsu Photonics) and the other is a near infrared camera (Goldeye G033 SWIR, Allied vision Technologies). The basic specifications of these cameras are shown in Table 2, and more details of the performance of the visible and IR cameras are presented in Oi et.al. (2015) and Yamasaki et.al. (2022), respectively.

The cameras are mounted on the exit port of the vertical or horizontal

spectrograph with a relay lens that demagnifies the image of two orthogonally polarized spectra made by the spectrograph (width of ~45mm) to fit the size of the detector. As a result, the spatial samplings along the slit direction are 0.14 and 0.43 arcsec/pixel for visible and IR camera, respectively. The camera starts the exposure in response to the trigger signal sent from the rotating stage of the waveplate and acquires a commanded number of frames continuously.

Table 1 Basic specifications of cameras

	ORCA flash 4.0 Hamamatsu Photonics	Goldeye G033 SWIR Allied vision Technologies
Wavelength [nm]	350 - 1000	1000 - 1700
Format [pixels]	2048 x 2048	640 x 512
Pixel size [mm]	6.5	15
Max. frame rate [s^{-1}]	100	301
AD bits	16	14

2.4 User interface and observation setup

Figure 4 display the user interface on the screen of the data acquisition PC. The observation software (dstpol) is written in IDL with some lower-level libraries written by C language on Windows. The control parameters to be set by observer are follows; selection of the camera, exposure time, number of images accumulated in each dataset, rotation speed of the waveplate, step size and number of steps for image scanning, repeat number of scanning, and output file ID and directory. Optionally quick look of demodulated IQUV spectra can be displayed on the screen in real time. The typical exposure time is 15-30 msec for on-disk observation and 50-200 msec for limb prominence observation, and the number of frames accumulated for one slit position is 100-200 frames. With such sequence, N/S of about $3x10^{-4}$ can be achieved in a few second for on-disk observations. A set of

modulated spectral images taken at one slit position is stored in a fits format file in the data acquisition PC with the information of DST attitude at the time.

It is necessary to take some datasets for later calibration after or before the sequence of the scientific observation. They are dark frames, number of spectral images of quiet regions by moving the solar image on the slit for making a flat field, dataset with a linear polarizer and hairlines placed in front of the slit, and dataset of a sunspot if it is available on the sun.

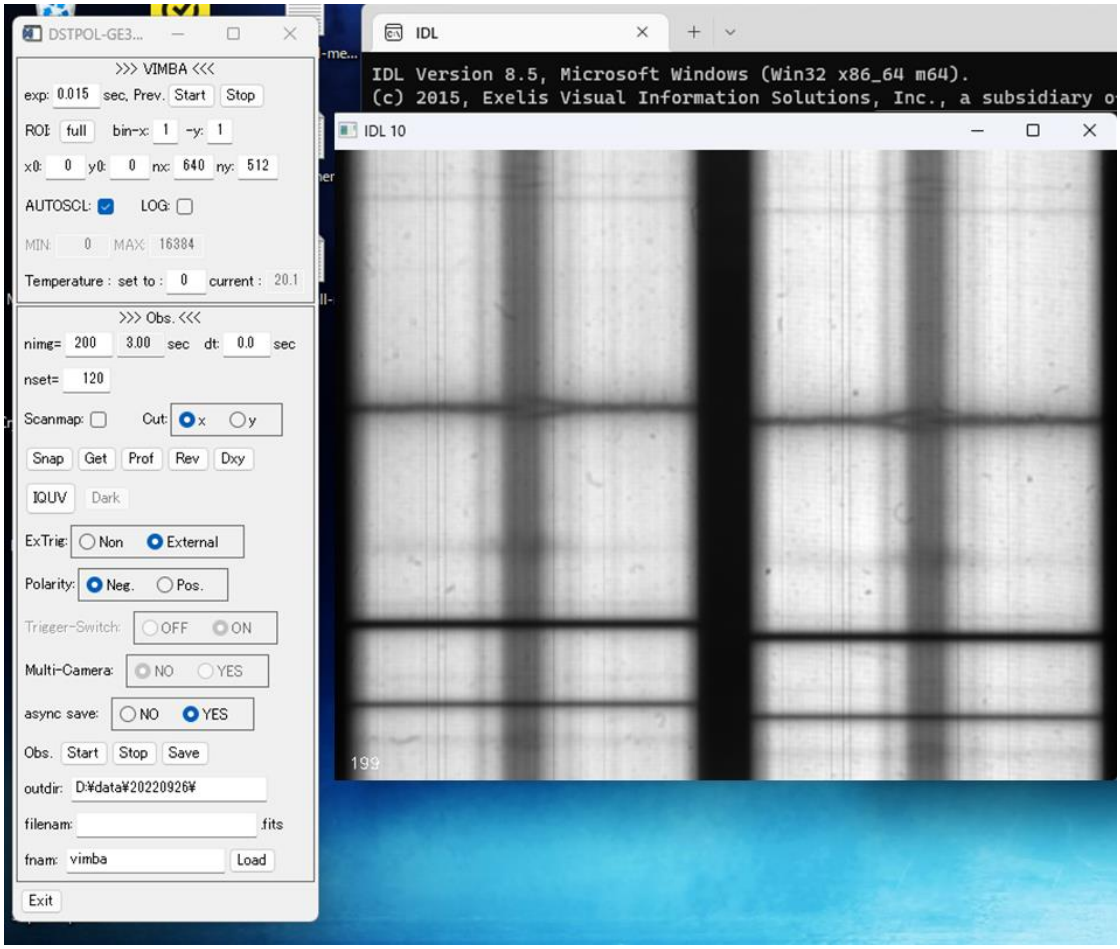

Figure 4. User interface screen on the data acquisition PC

Table 2 summarize the basic properties of the spectro-polarimeter

Table 2. Basic properties of the spectro-polarimeter

Operational wavelength	500 – 1100 nm
Wavelength resolution ($\lambda/\Delta\lambda$)	5 x 10^4 – 10^6 (flexible)
Field of view	120" (along slit) × <240" (scan)
Spatial sampling (along slit)	0.14"/pix (500-1000nm, with visible camera)
	0.43"/pix (1000-1100nm, with IR camera)
(scan step)	> 1"
(slit width)	0.32", 0.64", 1.28"
Exposure time (typical)	15 – 50 msec (on disk)
	50 – 200 msec (prominences)
Frequency of pol. modulation	0.5 – 4 sec (rotation period of waveplate)
Sensitivity	3 x 10^{-4} (200 frame integration)

3. Data reduction flow

The calibration procedure to deduce the Stokes I, Q, U and V spectra from the raw data is prepared as IDL programs. In our usual setup, the direction of dispersion is in vertical as seen in the bottom left of Figure 3. We call orthogonally polarized two spectra as 'left' and 'right' spectrum hereafter.

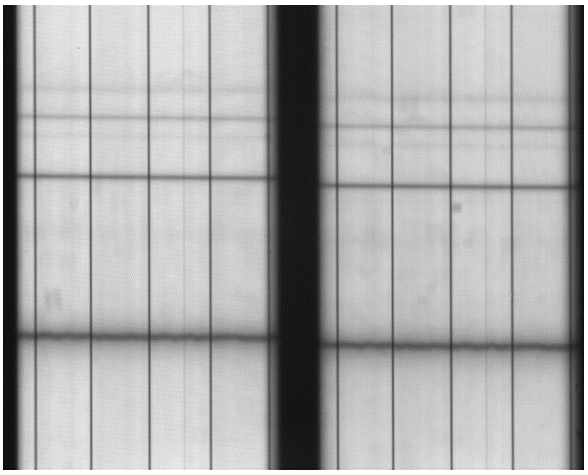

Figure 5. Spectral image taken with 5 hairlines on the slit of spectrograph.

The flow of the data reduction is as follows.

(1) Determine parameters necessary for aligning the left and right spectra using the spectrum image with the hairlines on the slit of spectrograph (shown in figure 5). The user selects crossing points of the hairline and absorption lines in the left and right spectra and a location for determining the continuum intensity level. Hairlines and absorption lines in both spectra are fit by 3rd order polynomials. The data of the polynomials is used for destretching and shifting each spectrum to precisely co-align them.

(2) Make flat images for the left and right spectra. Spectral images taken in quiet regions are summed up and averaged. After subtraction of the dark frame, the left and right spectra are extracted and aligned each other. Then absorption lines are removed from each spectrum by dividing by a spectral profile averaged in the slit direction.

(3) Prepare the spectral images for demodulation. After subtracting the dark frame from the raw data, left and right spectra are extracted and aligned to each other. Flat correction is applied on both spectra.

(4) Determine parameters necessary for demodulation. Using the dataset taken with a linear polarizer on the slit, the retardation of the waveplate and the ratio of the throughput of the left and right spectra are determined from the amplitudes of the intensity modulation in continuum. Also confirmed is the offset angle θ_0 of the waveplate with respect to the origin sensor of the rotation mechanism using R spectrum (described in the next step (5)) by browsing if polarization signals originating the Zeeman effect are not present in photospheric lines.

(5) Demodulate the set of spectral images to obtain preliminary Stokes spectra. Each left and right spectrum is demodulated separately by summing the sequence of images multiplied by 1, $\sin(4\theta_i + \theta_0)$, $\cos(4\theta_i + \theta_0)$, $\sin(2\theta_i + \theta_0)$ and $\cos(2\theta_i + \theta_0)$, then each of which produces the preliminary Stokes I, Q, U, V and R, respectively. Here θ_i is the angle of the waveplate at the instance of the i-th exposure and θ_0 is the

offset angle of the waveplate determined in step (4). In case of the ORCA camera, the exposure timing varies with the position on the detector due to the rolling shutter mechanism. This effect is taken into account in the demodulation. Optionally movements of spectra along the slit due to the tracking error during the data accumulation can be corrected by cross correlation method before the demodulation. The Stokes spectra obtained from the left and right spectra are combined after normalizing each spectrum by the continuum intensity or correcting the difference of throughput between them, thus a single set of Stokes I, Q, U, C and R is obtained. The magnitude of Stokes Q, U and V are divided by the theoretical modulation amplitudes calculated for a perfect linear and circular polarizations with the retardation of the waveplate. Finally, the Q-U frame is rotated so that the positive Stokes Q is aligned to the slit direction. The resultant Stokes I, Q, U, V are the Stokes parameters that entered to the slit of the spectrograph. An example of Stokes spectra thus obtained is shown in Figure 6(a). It is obvious that the Stokes Q and U have a significant bias in continuum, and features of spectral lines and a dark belt corresponding to a sunspot are visible. This is due to the instrumental polarization created in DST.

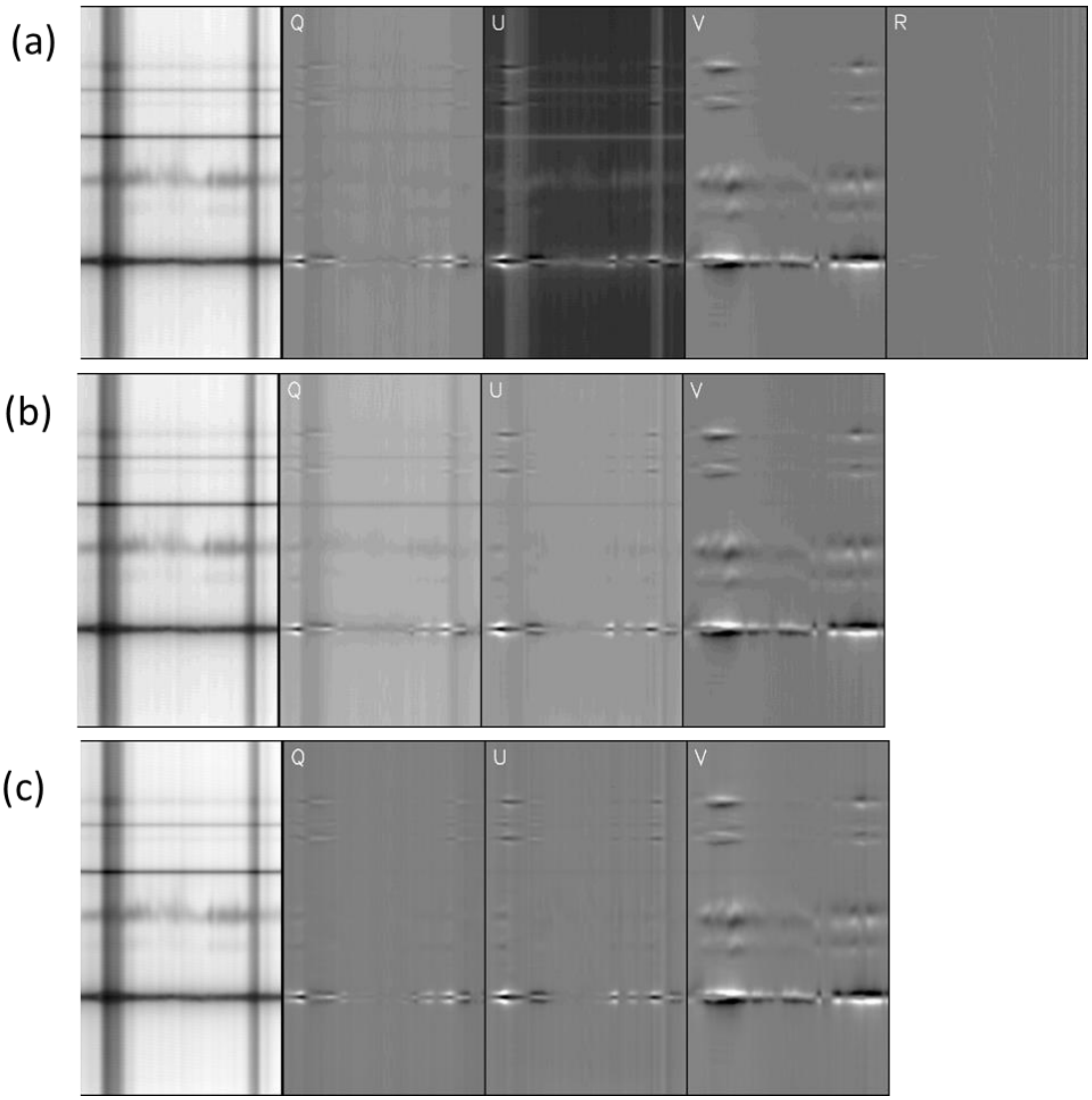

Figure 6. Stokes spectra after the demodulation (a), after the correction of instrumental polarization using the DST Mueller matrix model (b) and after the correction of I to QUV crosstalk (c). QUV are displayed in a scale of $\pm$5%.

(6) Correct the instrumental polarization by using the Mueller matrix of DST. As the initial guess of the Mueller matrix of DST, we adopt the model generated by Anan et al (2012). The Mueller matrix model of DST contains 5 basic parameters that characterizes the polarization of DST; i.e., diattenuation (p_N) and retardation (τ_N) of the Newton mirror (folding mirror between the primary and secondary mirror),

diattenuation (p_C) and retardation (τ_C) of the Coude mirror, and stray light (constant bias in intensity) (s). Since incidence angle of the light on the Newton and Coude mirrors is constant (45°) in time, p_N, τ_N, p_C and τ_C are functions of only on the wavelength, and they are tabulated in Anan's model. We calculated the DST Mueller matrix at the time of the observation by using these parameters, and then apply its invers to the Stokes spectra obtained by the demodulation. In case remaining cross talks are recognized in Zeeman sensitive lines (in sunspots if present), further tuning for the 5 parameters is performed so that the Stokes-V and Stokes-QU signals get anti-symmetric and symmetric profiles, respectively. Thus we obtained the most plausible Mueller matric model of DST as a function of telescope attitude or the time. Figure 6(b) shows the result of the correction for the instrumental polarization. Obviously Zeeman signals in spectral lines get more reasonable. However, we still see a bias in continuum and apparent contamination from Stokes-I in Q and U spectra.

(7) Correct the crosstalk from I to Q, U, V. We represent the correlations between Stokes I and Q, U, V spectra by linear functions obtained from regression of the data in a spectral area with no Zeeman signal, preferably, including atmospheric lines and sunspot continuum. The contributions of Stokes-I spectrum in each Stokes-Q, U, V spectrum are calculated from the linear relations and they are subtracted from the Q, U, V spectra. Figure 6(c) shows the result of this procedure. The bias in continuum and features of false lines in Stokes-Q, U, V are now disappeared.

(8) Remove fringes from Q, U, V spectra. When we focus on observational targets with a weak polarization signal, we often recognize periodic variations along the wavelength in Stokes Q, U. V spectra at a level of about 0.05%. Figure 7(a) shows an example of such pattern seen in the 1083 nm window. The fringe pattern is not stationary in time but changes rather rapidly with the attitude of the telescope. Therefor we

adopt an ad hoc method to mitigate this pattern, i.e., the periodic variation along the wavelength is fit with a sinusoidal curve using a continuum interval in the spectrum for each position along the slit, and then it is subtracted from the spectrum. At the same time, vertical stripes seen in Q, U, V spectra are also removed by subtracting a 3rd order polynomial fit of each spectrum. The result is shown in Figure 7(b), which demonstrates that the Stoles Q, U, V spectra get cleaner and the visibility of weak polarization signals are well improved.

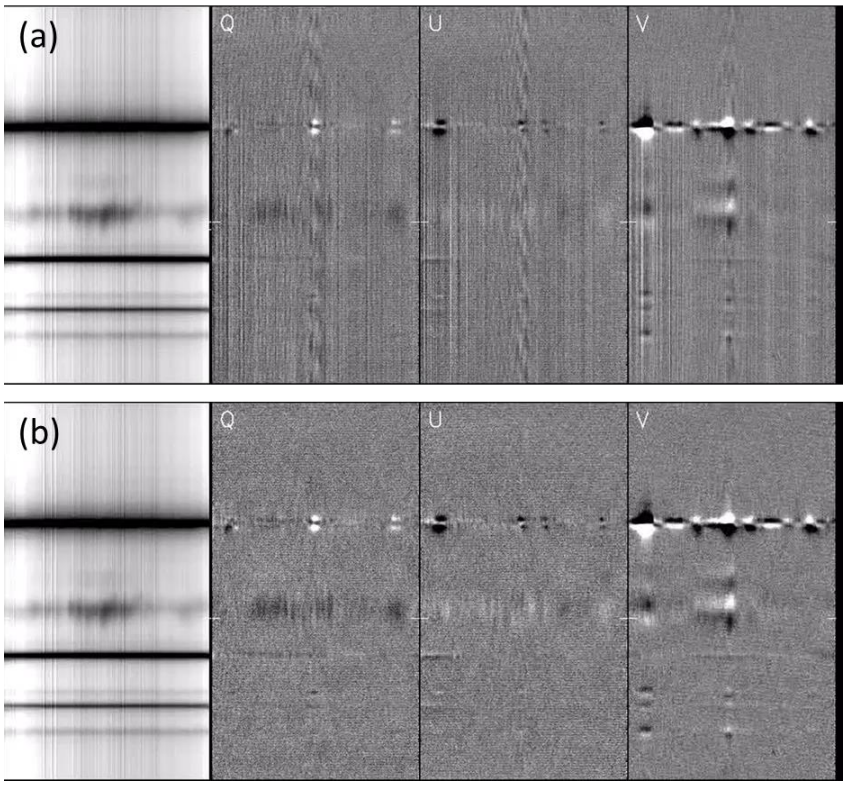

Figure 7. Stokes spectra after the correction of polarization crosstalk (a). (b) shows the result of defringing. QUV are displayed in a scale of ±0.2%.

(9) Make 2D maps and further analysis. Simple procedure to make 2D maps of I, Q, U and V intensities is available for the purpose of the quick look. Milen-Eddington inversion code to retrieve the magnetic field

from photospheric lines are also available. Further applications are up to the users.

4. Examples of data

In the followings of this section, some examples of the results from the new spectro-polarimeter are presented. Descriptions of the data are given in captions of each figure.

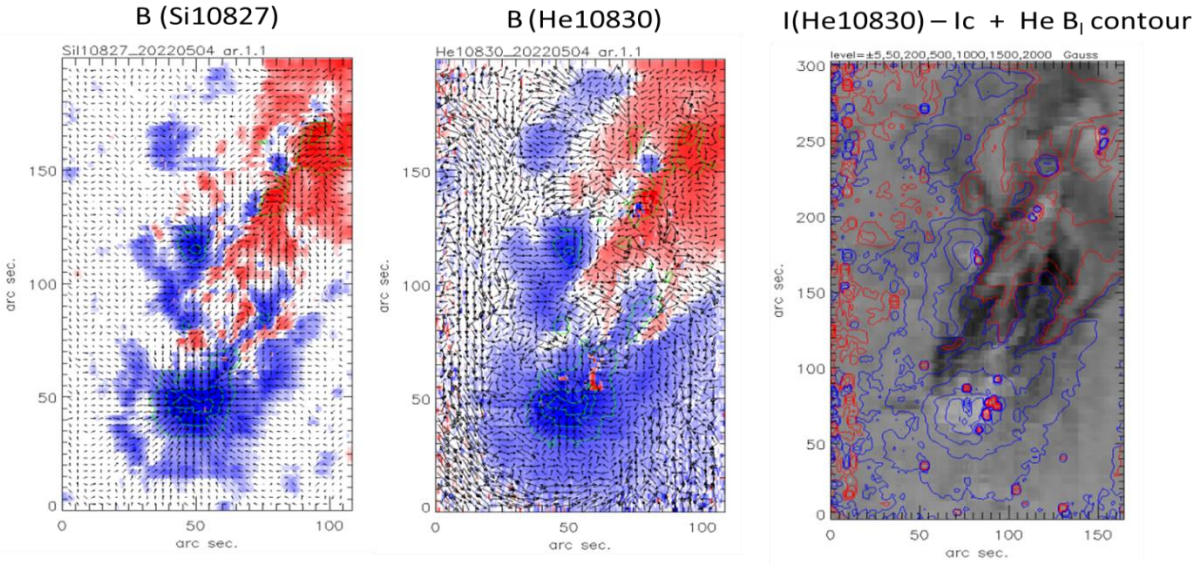

Figure 9. Magnetic field maps of an emerging flux region on 4 May 2022. Left: photospheric magnetic field obtained from Millen-Eddington inversion of SiI 1072.7 nm. Red and blue show positive and negative polarities of the longitudinal component and short lines show transversal component of the magnetic field. Middle: same as the left but of the chromospheric field obtained from HeI 1083 nm taking only Zeeman effect. Right: Intensity map of HeI 1083 nm overlaid by chromospheric longitudinal field with red and blue contours.

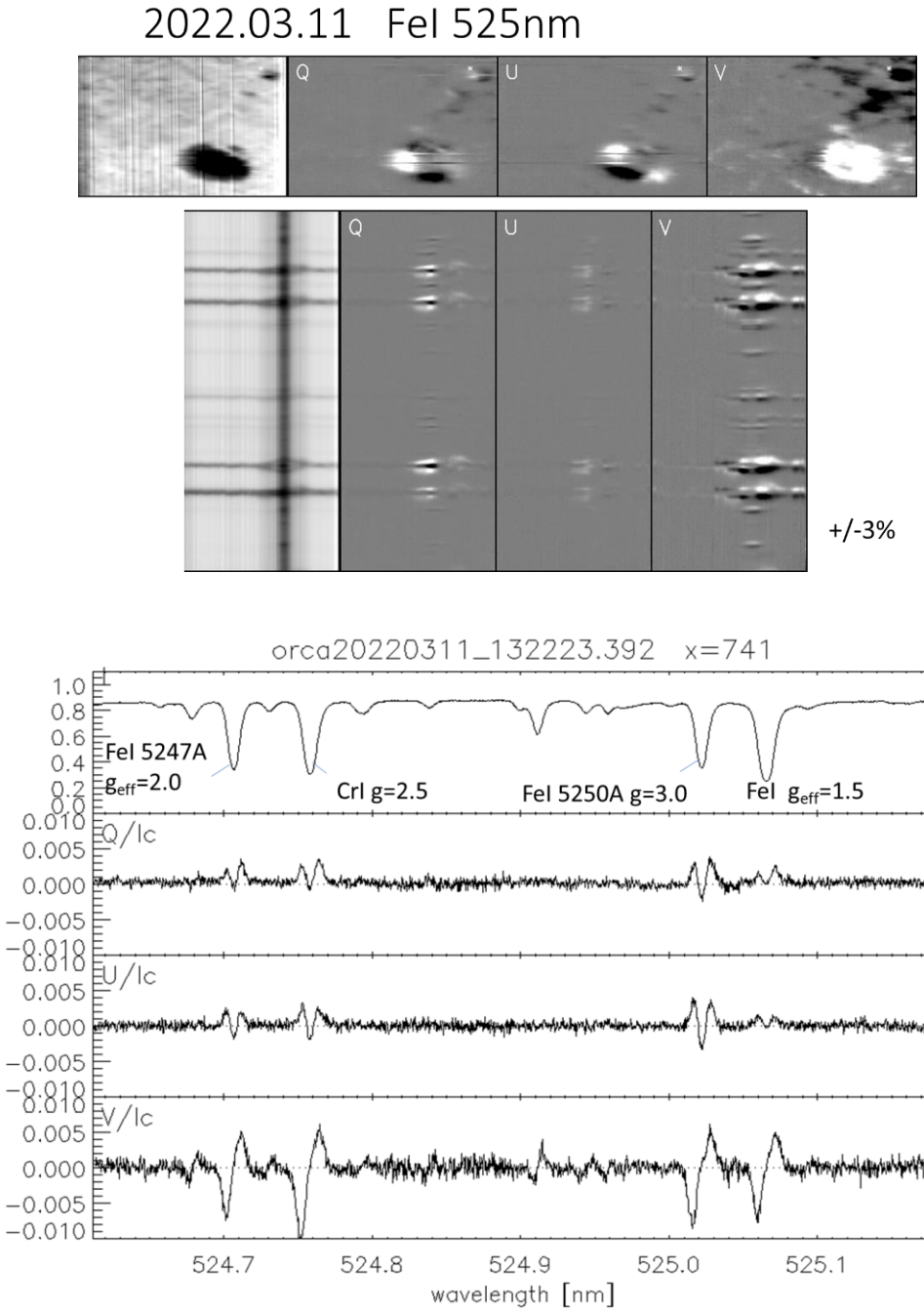

Figure 10. Results from the observation of a sunspot in FeI 525 nm window. Stokes spectra in upper panel are displayed in a scale of ±3%. Bottom panel shows Stokes profiles at a pixel in a weak field region to demonstrate the noise level in the spectra. Data was taken on 11 March 2022.

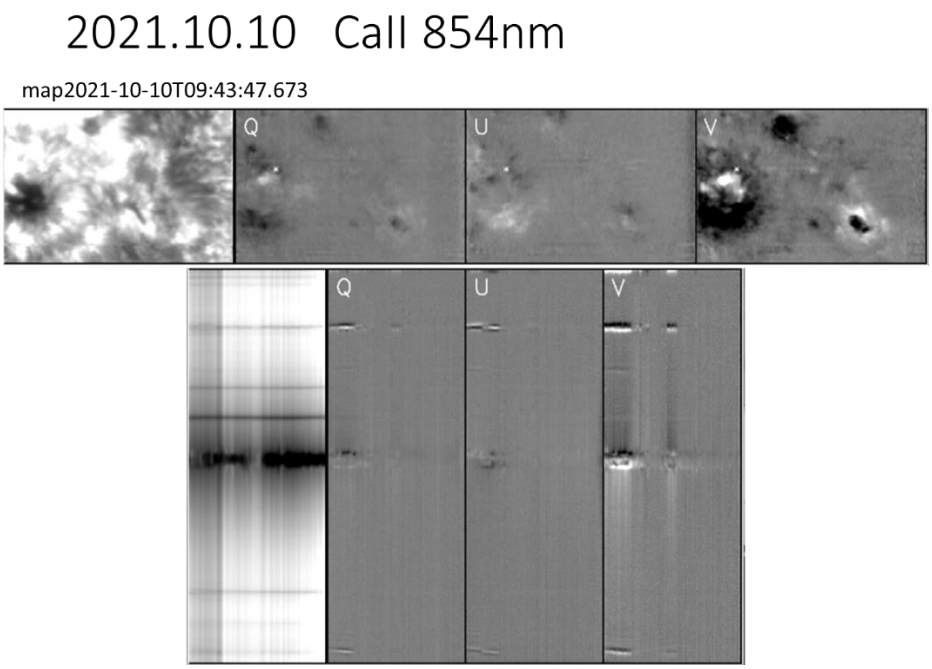

Figure 11. Observation of an active region in CaII 854.2 nm. Data was taken on 10 October 2021.

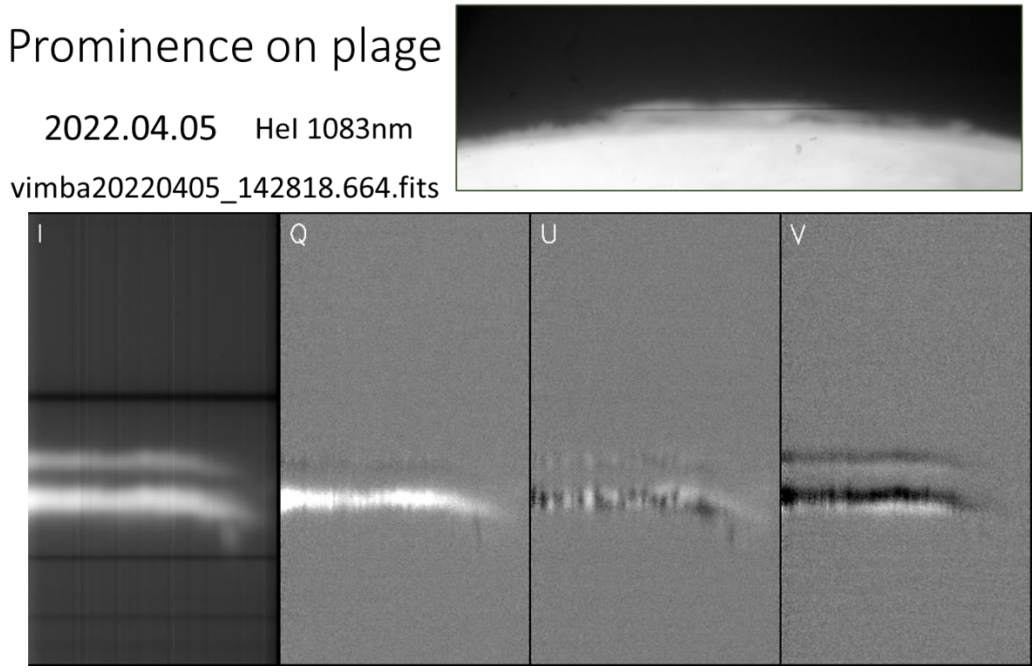

Figure 12. Stokes spectra from the observation of a low-lying prominence on the limb in HeI1083 nm. Data was taken on 5 May 2022. The prominence

was located in a plage region and the Stokes-V signal from the Zeeman effect infers the line of sight component of the magnetic field to be 18G.

5. Future prospect

So far, most observations with the new spectro-polarimeter have been conducted by using the vertical spectrograph of DST since the calibration of the instrumental polarization is well established for it. To use the horizontal spectrograph for multi-line observations, calibration of the polarizations of the image rotator in front of the entrance slit of the horizontal spectrograph is required. The Mueller matrix of the image rotator has been determined by Anan etal (2018), though we need further tuning. The polarimeter is also usable in combination with the adaptive optics (AO) system of the DST (Ichimoto etal 2022). We expect that the accuracy and spatial resolution of the polarimetric observations will be significantly improved by stabilizing the solar image on the slit during the data acquisition by AO. Mueller matrix of the AO system has also been measured by the Mueller matrix spectro-polarimeter (Ichimoto etal 2006). Although instrumental polarizations of the image rotator and AO are stronger than that of the DST and accurate calibrations are more challenging, procedures for correcting them will be implemented in the data reduction software soon.

The repeatability and the resolution of the image scanning is an issue to be improved in the current system. We plan to install a new scanning mechanism by using one of the folding mirrors in the AO system to improve the positioning accuracy better than 0.5arcsec. Another improvement of the current system is to enlarge the field of view along the slit. The length of the slit in current system is limited to 20 mm (=120 arcsec) by the size of the polarization analyzer and detectors. By using a larger polarizing beam splitter and an additional camera for one of the beams, it is possible to enlarge the FOV along the slit to that of the DST and the spectrographs, i.e., 300 arcsec.

The advantage of our spectro-polarimeter is in its flexibility in choosing the combination of wavelengths, spectral resolution and coverage, number of integration and time resolution, and opportunity for the observations. Extensive use of the new system stimulated by unique ideas from strong scientific motivations is highly expected.

Acknowledgements:
The authors thank the staff member of Hida observatory for their continuous support for our observation.

References:

- Anan, T., Ichimoto, K., Oi, A., et al. 2012, SPIE Proc., 8446, 84461C
- Anan, T., Huang, Y.-W., Nakatani, Y., et al. 2018, PASJ, 70, 102
- Ichimoto, K., Shinoda, K., Yamamoto, T., Kiyohara, J.: 2006, Publ. Natl. Astron. Obs. Japan 8, 11.
- Ichimoto, K., Nakatani, Y., Ueno, S., Kimura, G., Miura, T., Eriguchi, A. and Takeyama, N., 2022, Tech. Rep. from Astron. Obs. Grad. School of Science, Kyoto Univ., Vol.6-1
- Kiyohara, J., UeNo, S., Kitai, R., et al. 2004, SPIE Proc., 5492, 1778
- Nakai, Y. and Hattori, A. 1985, Mem. Faculty of Science, Kyoto University, Ser. Physics, Astrophys. Geophys. and Chem., 36, 385
- Oi, A., Anan, T., Sano, M., Ichimoto, K. and Nagata, S., 2015, Tech. Rep. from Astron. Obs. Grad. School of Science, Kyoto Univ., Vol.3-1
- Yamasaki, D., Huang, Y. W., Hashimoto, Y. et al. 2022, Tech. Rep. from Astron. Obs. Grad. School of Science, Kyoto Univ., Vol.6-2